

Inverse Least-Squares Modeling of Induced Polarization and Resistivity Data to Explore Copper Deposits in the Sarbisheh Ophiolites, Iran

Adnan Sharafi, Hamid Sarkheil, Mohammad Kazem Hafizi

Abstract— Since the resistivity and induced polarization, methods have an important role for exploration of copper mineralization. Kuh Kheyri area is located south of Sarbisheh in south Khorasan province. This area is located in sheet 1:250000 of Brijand and 1:100000 Sahlabad. The existence of volcanic rocks like Andesite, and the metallic mineralization with small to large sizes in this type of rocks, has made this area quite remarkable of having mining potential. Since surface exploration, methods like geology and geochemistry are not solely capable of determination of depth, direction and dip of mineralization, the geophysical methods can be effective. By taking into consideration the physical changes of existing rocks in the area and also the sulfide mineralization in it, the Induced polarization and resistivity method was used for determination of those areas having low resistivity, and high induced polarization was carried out to distinguish the anomaly zones. The array used is Dipole-Dipole with 40 meters electrode spacing and 20 meters bond spacing. Four pseudo sections with 100 meters distance of each other as parallel and also two perpendicularly pseudo sections with 50 meters distance from each other are designed and carried out. The total 1218 Induced polarization and electrical resistivity points was measured. The pseudo section of IP and RS was measured and least-squares inversion modeling sections with topographic correction was done with Res2dinv software and then the results was explained and analyzed. The studies has shown that according to surface geological evidences compared with induced polarization sections and resistivity, the maximum amount of chargeability in 3sections with minimum resistivity have good relative accordance and in the other 3 sections, the resistivity is high probably due to the open spaces or silicification of mineralizes zones in this 3 sections, causing the increase of resistivity. In general, according to surface geological and geophysical results, this area has a very good potential for copper mineralization.

Index Terms— Copper, Induced Polarization, Least-Squares Inversion, Resistivity, Kuh Khayri.

I. INTRODUCTION

Electrical methods comprise a multiplicity of separate techniques that employ differing instruments and procedures, have variable exploration depth and lateral resolution, and are known by a large lexicon of names and acronyms describing techniques and their variants. Electrical methods can be described in five classes [1]: (1) direct current resistivity, (2) electromagnetic, (3) mise-a-la-masse, (4) induced polarization, and (5) self-potential.

Manuscript Received on October 22, 2014.

Adnan Sharafi, Islamic Azad University, North Tehran Branch, Tehran, Iran.

Hamid Sarkheil, Department of Environmental Engineering, University of Environment, Karaj, Iran.

Mohammad-Kazem Hafizi, Institute of Geophysics, University of Tehran, Tehran, Iran.

In spite of all the variants, measurements fundamentally are of the Earth's electrical impedance or relate to changes in impedance. Electrical methods have broad application to mineral and geo environmental problems: they may be used to identify sulfide minerals, are directly applicable to hydrologic investigations, and can be used to identify structures and lithologies [1]. Direct current resistivity methods measure Earth resistivity (the inverse of conductivity) using a direct or low frequency alternating current source. Rocks are electrically conductive as consequences of ionic migration in pore space water and more rarely, electronic conduction through metallic luster minerals. Because metallic luster minerals typically do not provide long continuous circuit paths for conduction in the host rock, bulk-rock resistivities are almost always controlled by water content and dissolved ionic species present. High porosity causes low resistivity in water-saturated rocks. Direct current techniques have application to a variety of mineral exploration and geo-environmental considerations related to various ore deposit types. Massive sulfide deposits are a direct low resistivity target, whereas clay alteration assemblages are an indirect low resistivity target within and around many hydrothermal systems. The wide range of earth material resistivities also makes the method applicable to identification of lithologies and structures that may control mineralization. Acid mine waste, because of high hydrogen ion mobility, provides a more conductive target than solutions containing equivalent concentrations of neutral salts [2], [3]. The induced polarization method provides a measure of polarizable minerals (metallic-luster sulfide minerals, clays, and zeolites) within water-bearing pore spaces of rocks. Polarizable minerals, in order to be detected, must present an active surface to pore water. Because induced polarization responses relate to active surface areas within rocks, disseminated sulfide minerals provide a much better target for this method than massive sulfide deposits, although in practice most massive sulfide deposits have significant gangue and have measurable induced polarization. Induced polarization has found its greatest application in exploration for disseminated sulfide ore, where it may detect as little as 0.5 volume percent total metallic luster sulfide minerals [4]. In geo-environmental studies, induced polarization surveys are principally used to identify sulfide minerals, but it may have other applications, such as outlining clay aquitards that can control mine effluent flow [5]. In this study, resistivity and induced polarization surveys were carried out over a portion of the Zamin K. Z. and Zharf Negar K. groups, during February, March, and August 2014. This study area is located to the immediate northeast of Iran.

II. STUDY AREA AND GEOLOGY SETTING

This study area is located at about 25Km south-west of Sarbisheh of Khorasan-e-Jonobi province. This region is a part of Birjand 1:250000 and 1:100000 Sahlabad geological sheets (Fig. 1 and Table No. 1).

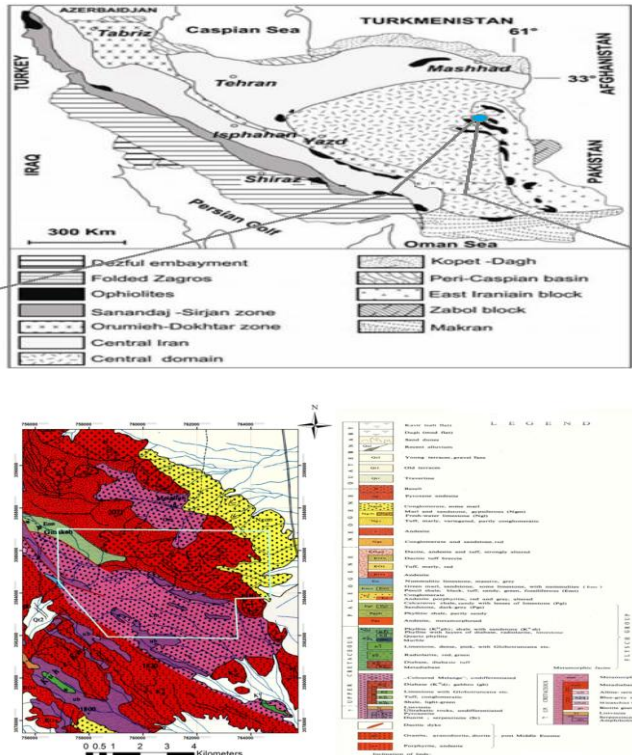


Fig. 1: Location of Study Area above Birjand 1:250000 Geological Sheet

Table 1: Longitude and Latitude of Sarbisheh Exploration Region of Khorasan, Iran

No.	X(m)	Y(m)
A	756826	3587015
B	764648	3586914
C	764726	3583786
D	763421	3583732
E	763513	3581854
F	758688	3581937
G	756858	3584534

The important geologic features of Eastern Iran is the ophiolite-flysch zone, these regions are one of the most particular parts of the Alpine belt. In the eastern part of the Lut block, near the Iran-Afghanistan border, there is an oceanic basin (Sistan Ocean), separating segments of the Alpine Belt [6]. The ophiolites are typically the signature of an oceanic basin. Iranian ophiolites are part of the Middle Eastern Ophiolite Chain, which extends from Cyprus through Turkey, Syria and Iran into Oman. Takin (1972) and Stocklin (1968, 1974) divided the Iranian ophiolites into four groups [7], [8] and [9]:

I) ophiolites of the Zagros, typically small and mixed with abundant mélangé.

II) ophiolites of the Rezaiyeh-Esphandagheh orogenic belt, including complex at Khoy, Kermanshah, Neyriz, and Esphandagheh.

III) ophiolites that mark the boundaries of the Central Iranian plate, located at Nain, Birjand, and Iranshahr.

IV) ophiolites of the Alborz Range, located at Mashhad, Sabzevar and Rasht (Talesh ophiolite). The Birjand ophiolitic range (studied area) is classified in third group and situated within the Sistan suture zone in Sahlabad province.

The ophiolites of Iran may be subdivided into two age groups: the less abundant Paleozoic and more abundant Mesozoic ophiolites (Arvin & Robinson, 1994). Lippard et al. (1986) suggested emplacement ages of Pre- Paleocene for all of the Mesozoic ophiolite complexes [9], [10], whereas Babazadeh and De Wever (2004) reported an emplacement before Maastrichtian for the ophiolites in the Soulabest area (Gazik province) [11]. In eastern Iran, the studied area (Sistan ocean in the Sahlabad province), Tirrul et al. (1983) stated that the oldest rocks separating the Lut block from the Afghan block are attributed to Upper Cretaceous [12]. However, the above results of the radiolarites within the ophiolite range, indicate that the oldest rocks belong to late Early Cretaceous (Late Albian) to early Late Cretaceous (Albian-Cenomanian) age, and the oceanic opening took place in Early Cretaceous. Moreover, the Late Albian radiolarian fauna in Sahlabad province (eastern part of Lut block) could be correlated with the radiolarian assemblage II of Gazik province (western part of Afghan block) and the Samail radiolarites [13], [11]. The oceanic crust was later emplaced before the Upper Cretaceous resedimented facies (flysch-type sediments) in the Fanud Unit. This is the first finding of Early Cretaceous radiolarian in Sahlabad province (eastern part of Lut block). The studied faunal assemblage was confirmed from deep marine basin and can be related to Tethyan radiolarites [14]. The most impressive geological feature in study area is the upper cretaceous sequences, consisting of diabase, gabbro, limestone, tuff, shale and dunite. The oldest geological unit in the area is the colored mélangé unit, which has an upper Cretaceous age. Argillization, sericitization, propylitization and silicification are the most common types of hydrothermal alterations in the area. Copper occurrence are numerous, some of them being exploited in the ancient times.

III. RESULT AND DISCUSSION

In order to interpret the geophysical data, Res 2DINV&3DINV [15],[16] computer program was used to perform a 2D inverse modeling for resistivity and induced polarization data along P₁, P₂, P₃, P₄, P₅ and P₆ profiles So, with the D01, D02, D03, D04, D05 and D06 have been named. (Fig. 2).

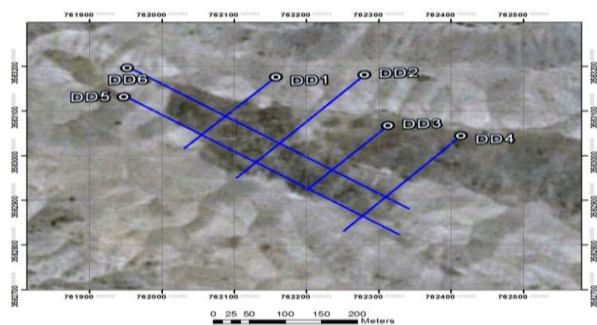


Fig. 2: Location of P1, P2, P3, P4, P5 and P6 Profiles on



Studied Area (Khuh Khayri - Sarbisheh Region of Khorasan, Iran)

A geoelectrical measurement is carried out by recording the electrical potential arising from current input into the ground with the purpose of achieving information on the resistivity structure in the ground [17]. In a homogeneous ground (half space) the current flow, radially out from the current source and the arising. Equipotential surfaces run perpendicular to the current flow lines and form half spheres (Fig. 3a). In the common situation with both a current source and a current sink the current flow lines and the equipotential surfaces become more complex (Fig. 3b). In reality the current flow lines and the equipotential lines will form an even more complex pattern as the current flow lines will bend at boundaries, where the resistivities change. Geoelectrical data are commonly expressed as apparent resistivities;

$$\rho_a = \frac{\Delta V}{I} K \tag{1}$$

Where ΔV ; is the measured potential, I ; is the transmitted current, and K ; is the geometrical factor expressed as:

$$K = 2\pi \left[\frac{1}{|r_A - r_M|} - \frac{1}{|r_A - r_N|} - \frac{1}{|r_B - r_M|} + \frac{1}{|r_B - r_N|} \right] \tag{2}$$

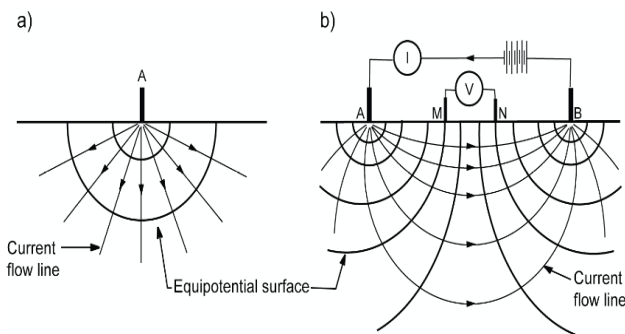


Fig. 3: Simplified Current Flow Lines and Equipotential Surfaces Arising from (a) A Single Current Source and from (b) A Set of Current Electrodes (A Current Source and Sink) [18]

A. Least-Squares Inversion Modeling

The inversion routine used by the software is based on the smoothness constrained least-squares method [19], [20]. The smoothness-constrained least-squares method is based on the following equation:

$$(J^T J + uF) d = J^T g \tag{1}$$

- Where $F = f_x f_x^T + f_z f_z^T$
- f_x = horizontal flatness filter
- f_z = vertical flatness filter
- J = matrix of partial derivatives
- u = damping factor
- d = model perturbation vector
- g = discrepancy vector

One advantage of this method is that the damping factor and flatness filters can be adjusted to suit different types of data [21]. Change of damping factor with depth - Since the resolution of the resistivity method decreases exponentially with depth, the damping factor used in the inversion least-squares method is normally also increased with each

deeper layer. This is done in order to stabilize the inversion process. Normally, the damping factor is increased by 1.05 times with each deeper layer, but you can change it. Use a larger value if the model shows unnatural oscillations in the resistivity values in the lower sections. This will help to suppress the oscillations. Also, select the choice to allow the program to determine the value to increase the damping factor with depth automatically. This might be a good choice if the thickness of the layers is much thinner than the default values, for example if you had reduced the unit electrode spacing by half in the data file in order to produce a model with smaller model blocks [22].

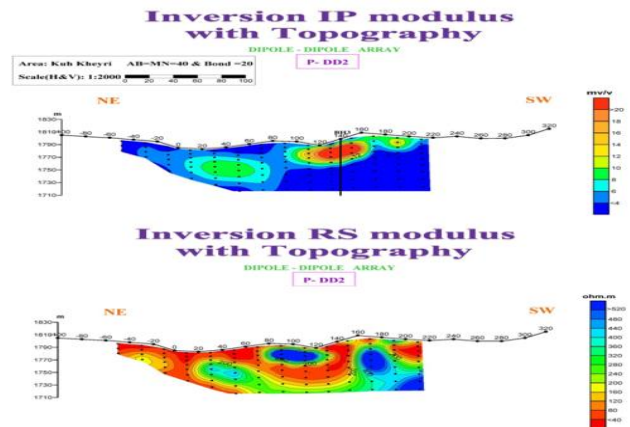


Fig. 4: 2D Resistivity Models Obtained by Inversion of RES and IP Data; Chargeability Section (Lower), Resistivity Section (Upper), Profile No. 2.

As you can see in figure No. 4, the resistivity decreases to a value less than 40 ohm-m from the lateral of an anomaly pocket to an approximate distance of 140 meters in the downstream along the profiles P₂ which is nearly parallel to axis of area. The chargeability model proves the mineralized zone along the profile by increasing of the value of chargeability in the same location. As it is well illustrated in this figure, the anomaly zone is depicted as a low resistivity zone and high chargeability zone in the middle of the profile (Fig. 4).

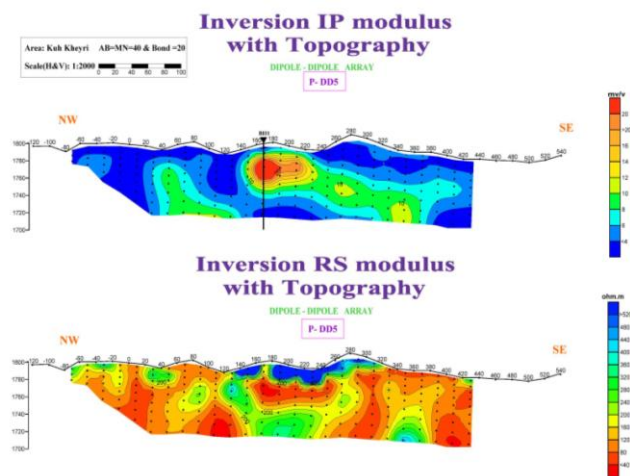


Fig. 5: 2D Resistivity Models Obtained by Inversion of RES and IP Data; Chargeability Section (Lower), Resistivity Section (Upper), Profile No. 5

Figure No. 5 indicates another anomaly region to an approximate distance of 170 meters in the downstream along the profiles P5 that is nearly parallel to axis of area. A low resistivity zone and high induced polarization zone in the center part of the profiles are clearly illustrated due to the outcrop is located at above of this part of profiles (Fig. 5).

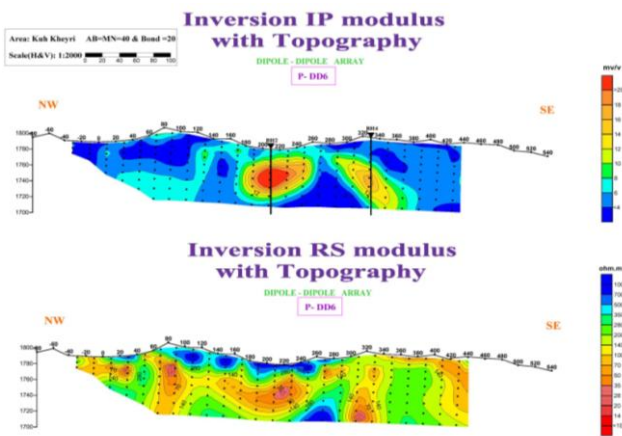


Fig. 6: 2D Resistivity Models Obtained by Inversion of RES and IP Data; Chargeability Section (Lower), Resistivity Section (Upper), Profile No. 6

Figure No. 6 indicates another two geophysical anomalies region to an approximate distance of 210 and 330 meters in the downstream along the profiles P₆. A low resistivity zone and high induced polarization zone in the center part of the profiles are clearly illustrated due to the outcrop is located at above of this part of profiles (Fig. 6). On other profiles (P₁, P₃ and P₄) cannot be expected the presence of economic copper anomalies.

IV. CONCLUSIONS

This study investigated the new interpretation method for inverse modeling from geoelectrical data for example in copper mine, located at the south-east of Khorasan, using dipole-dipole method, in addition, the necessary geoelectrical sections along different profiles covering the study area were provided by performing a numerical modeling on resistivity and induced polarization data. The geoelectrical setting provided by inverse modeling of dipole-dipole data are in good agreement with outcrops and geological sections. The most important criteria are the results obtained in this study provided reliable results for more possible area for copper ore exploration. It is important to conduct this research in terms of infield work because it can help members to join the geophysical community to improve understanding of the obtained geophysical results. In addition, the imaging (models) and geological analysis methods applied in this study was able to increase the validity and reliability of results in the field of geophysical imaging subsurface. So that anomalies identified in this phase of the study can be, illustrate the next stage of exploration program that is in compliance of geological studies in this region and can be introduced an integrated inverse modeling for induced polarization and electrical resistivity data.

ACKNOWLEDGMENT

The authors should like to acknowledge the financial support provided by Zamin K. Z. and Zharf Negar K. companies.

REFERENCES

1. Van Blaricom, Richard, (1980) - Practical geophysics: Northwest Mining Association, 303 p.
2. Christensen NB, Sorensen KI, (1998) - Surface and borehole electric and electromagnetic methods for hydrogeological investigations. – European Journal of Environmental and Engineering Geophysics 3: 75–90.
3. Sorensen K.I., Auken E., Christensen N.B., Pellerin L., (2005)- An Integrated Approach for Hydrogeophysical Investigations: New Technologies and a Case History. – In Butler D K (ed.) Near-Surface Geophysics 2, Investigations in Geophysics 13: 585–603. Society of Exploration Geophysics.
4. Sumner, J.S., (1976) - Principles of induced polarization for geophysical exploration: Elsevier, 277 p.
5. Osiensky, I.L., and Donaldson, P.R., (1994) - A modified mise-a-la-masse method for contaminant plume delineation: Ground Water, v. 32, no. 3, p. 448-457.
6. Takin, M., (1972) - Iranian geology and continental drift in the Middle East. Nature, 235: 147-150.
7. Stöcklin, J., (1968) - Structural history and tectonics of Iran : A review. American Association of Petroleum Geologists Bulletin, 52: 1229-1258.
8. Stöcklin, J., (1974) - Possible ancient continental margin in Iran. In: Burk, C. A. and Drake, C. L., (eds). The geology of continental margins. Berlin, Springer, 873-887.
9. Arvin, M. and Robinson, P. T., (1994) - The petrogenesis and tectonic setting of lavas from the Baft ophiolitic mélange, southwest of Kerman, Iran. Canadian Journal of Earth Sciences, 31 : 824-834.
10. Lippard, S. J., Shelton, A. W., and Gass, I. G., (1986) – The ophiolite of northern Oman. Geological Society of London, Memoir 11.
11. Babazadeh, S. A. and De Wever, P., (2004a) – Radiolarian Cretaceous age of Soulabest radiolarites in ophiolite suite of eastern Iran. Bulletin de la société géologique de France, 175(2): 121-129.
12. Tirrul, R., R. Bell, R.J. Griffis, and V. E., Camp, (1983) – The Sistan suture zone of eastern Iran. Geological Society of America Bulletin, 94 : 134-150.
13. Beurrier, M., C., Bourdillon-De-Grissac, P. De Wever and Lescuyer, J. L., (1987) - Biostratigraphie des radiolarites associées aux volcanites ophiolitiques de la nappe de Samail (Sultanat d'Oman) : conséquences tectogénétiques. Comptes Rendus de l'Académie des Sciences, Paris, 304 (2) : 907-910.
14. Babazadeh, S. A. & De Wever, P., (2004b) - Early Cretaceous radiolarian assemblages from radiolarites in the Sistan Suture (eastern Iran). Geodiversitas, 26(2) : 185-206.
15. ABEM. (1995) -Instruction manual for Terameter SAS 4000, ABEM Instrument AB, 91 p.
16. Lock M. H., (2002) – User manual for Res2dinv&3dinv Ver.3.5. Geotomo softwar.
17. Hoover, D.B., Heran, W.D., and Hill, P.L., eds., (1992) - The geophysical expression of selected mineral deposit models: U.S. Geological Survey Open-file Report 92-557, 129 p.
18. Sarkheil, H., Hassani, H., (2009) - A new design for geoelectric surveying and inverse 1D and 2D modeling: the case of Karongah lead-zinc mine, Kerman, Iran, 9th International Multidisciplinary Scientific Geo-Conference & EXPO SGEM 2009, 14-19 June 2009, Bulgaria, pp. 637-641.
19. deGroot-Hedlin, C. and Constable, S., (1990) - Occam's inversion to generate smooth, two-dimensional models form magnetotelluric data. Geophysics, 55, 1613-1624.
20. Sasaki, Y., (1992) - Resolution of resistivity tomography inferred from numerical simulation. Geophysical Prospecting, 40, 453-464.
21. Loke, M.H., (2001) - Tutorial : 2-D and 3-D electrical imaging surveys. Geotomo Software, Malaysia.
22. Loke, M.H., Acworth, I. and Dahlin, T., (2003) - A comparison of smooth and blocky inversion methods in 2D electrical imaging surveys. Exploration Geophysics, 34, 182-187.